Theoretical Study of Volume Changes Accompanying Xenon−Lysozyme Binding: Implications for the Molecular Mechanism of Pressure Reversal of Anesthesia

Takashi Imai,*,† Hideto Isogai,‡ Tomoyoshi Seto,‡,§ Andriy Kovalenko,|| and Fumio Hirata⊥

Departments of Bioscience and Bioinformatics and Applied Chemistry, Ritsumeikan University, Kusatsu, Shiga 525-8577, Japan, Department of Anesthesiology, Shiga University of Medical Science, Otsu, Shiga 520-2192, Japan, National Institute for Nanotechnology, National Research Council of Canada, and Department of Mechanical Engineering, University of Alberta, Edmonton, Alberta T6G 2V4, Canada, and Department of Theoretical Studies, Institute for Molecular Science, Okazaki, Aichi 444-8585, Japan

Received: November 3, 2005; In Final Form: March 24, 2006

The change in partial molar volume (PMV) accompanying the xenon−lysozyme binding was investigated for elucidating the molecular mechanism of the pressure reversal of general anesthesia, using the three-dimensional reference interaction site model theory of molecular solvation. An increase of the PMV from xenon binding to the substrate binding site of lysozyme was found, and the binding is suppressed by pressure, while the internal site binding did not change the PMV. The PMV change was analyzed by decomposing it into several contributions from geometry and hydration. We also analyzed the hydration change due to the binding. From the results, we draw a molecular picture of the PMV change accompanying xenon−lysozyme binding, which gives a possible mechanism of pressure reversal of anesthesia.

1. Introduction

The pressure reversal of general anesthesia has been considered to provide a key to elucidating the molecular mechanism of general anesthesia.[1−6] Early workers believed that anesthetics acted nonspecifically on hydrophobic lipid components of cells. However, recent studies have demonstrated that anesthetics interact with specific sites of transmembrane proteins such as ion channels, which regulate signal transduction.[7−9] In those studies, the anesthetic−protein binding is considered as a physicochemical or thermodynamic process at the molecular level. If this is the case, then the pressure reversal of general anesthesia should be explained in terms of thermodynamics.

The dependence of the anesthetic−protein binding constant K on pressure P is related to the change in partial molar volume (PMV) accompanying the binding $\Delta\bar{V} = \bar{V}_{\mathrm{complex}} - (\bar{V}_{\mathrm{protein}} + \bar{V}_{\mathrm{anesthetic}})$

$$\left(\frac{\partial \ln K}{\partial P}\right)_T = -\frac{\Delta\bar{V}}{RT} \tag{1}$$

where R is the gas constant and T is the temperature. Under the framework of thermodynamics, the pressure reversal of general anesthesia should be reflected by the anesthetic−protein binding with the total PMV increase. In fact, Ueda and Mashimo[4] showed that the binding of diethyl ether (anesthetic) to bovine serum albumin (model lipid-free protein) expanded the PMV by 295 cm^3/mol. For another protein, firefly luciferase, it was found that the binding of halothane (anesthetic) with low affinity ($K_D \approx$ millimolar) increased the PMV by 3.93 cm^3/mol, whereas the binding of myristate (specific inhibitor) with high affinity ($K_D \approx$ micromolar) decreased the PMV by 7.66 cm^3/mol.[6]

Eyring et al.[1] and Ueda and Mashimo[4] proposed that the volume expansion of proteins is due mainly to the release of "freezing" water molecules on the protein surface. Water molecules around an ionic species become denser compared to the bulk due to the strong electrostatic interactions, and consequently the PMV is reduced. The phenomenon is known as electrostriction.[10] They suggested that the binding of anesthetics releases such "electrostricted" water molecules from the vicinity of ionic residues of proteins. However, no experimental evidence for the electrostriction hypothesis has been presented. Thus the molecular mechanism of the volume increase as well as the dehydration accompanying the anesthetic binding remain unanswered questions.

It is useful in understanding the PMV change to decompose the PMV into several contributions[11]

$$\bar{V} = V_{\mathrm{id}} + V_{\mathrm{W}} + V_{\mathrm{V}} + V_{\mathrm{T}} + V_{\mathrm{I}} \tag{2}$$

where the components are identified as follows. V_{id} is the ideal volume contribution from the translational degrees of freedom of a molecule. The next two components are the geometric volume contributions: V_{W} is the van der Waals volume, and V_{V} is the void volume owing to structural voids within the solvent-inaccessible core. The last two components are the solvation effects on the PMV. V_{T} is the so-called thermal volume that results from thermally induced molecular fluctuations between the solute and the solvent molecules. It has been introduced to explain the distinction between the PMV and the molecular volume ($V_{\mathrm{W}} + V_{\mathrm{V}}$) for small nonpolar molecules.[11] V_{I} is the interaction volume representing the change in the solvent volume by the intermolecular electrostatic interaction between the solute and the solvent molecules. Accordingly, it is directly related to the electrostriction effect. Although this decomposition provides a molecular picture of the PMV, it was

* Author to whom correspondence should be addressed. E-mail: t-imai@is.ritsumei.ac.jp.
† Department of Bioscience and Bioinformatics, Ritsumeikan University.
‡ Department of Applied Chemistry, Ritsumeikan University.
§ Shiga University of Medical Science.
|| University of Alberta.
⊥ Institute for Molecular Science.

10.1021/jp056346j CCC: $33.50
Published on Web 05/25/2006

difficult for experiments to resolve the last two contributions, because they both reflect the solvation structure and are closely related to each other. Direct resolution of these solvation effects without empirical assumption or ambiguity is provided by the reference interaction site model (RISM) theory, in particular and its three-dimensional version (3D-RISM) that can decompose the two contributions rationally.

The 3D-RISM theory[12−15] is a recently developed statistical-mechanical theory of molecular solvation and has been successfully applied to solvation thermodynamics of proteins.[16] Moreover, the 3D-RISM theory coupled with the Kirkwood−Buff (KB) theory[17] has been found to provide quantitatively reasonable results for the PMV of various molecules including amino acids[18] and proteins.[16] The theory has been also used in the decomposition expressed in eq 2 with great success.[19−21] The 3D-RISM-KB theory is a promising candidate for analyzing the volumetric properties associated with the anesthetic−protein interactions to investigate pressure reversal mechanisms of general anesthesia.

Recently, Isogai et al.[22] showed the substrate binding site of hen egg white lysozyme can be a model site of the pressure reversal of general anesthesia. They demonstrated using docking simulations that the binding of xenon, one of the simplest anesthetics, to the site was energetically destabilized under high pressure. We choose the xenon−lysozyme system as a pressure reversal model, because the three-dimensional structure of the protein in solution has been resolved[23] and the xenon binding sites have been estimated by docking simulations.[22]

In this study, we first apply the 3D-RISM-KB theory to the xenon−lysozyme binding as a model system of the pressure reversal of anesthesia. Second, we analyze the PMV change accompanying the xenon binding based on the decomposition of eq 2 to investigate the molecular mechanisms of PMV change. Third, we also infer the hydration of anesthetic binding sites to obtain a physical picture of anesthetic binding. From these analyses, we propose a new hypothesis revealing the molecular mechanism of the pressure reversal of general anesthesia.

2. Methods

2.1. Theoretical Definition of Volume Components. The volume components in eq 2 can be obtained from the 3D-RISM-KB theory and from the geometric volume calculation.[19−21] The ideal volume V_{id} is the ideal gas contribution to the PMV and is naturally included in the 3D-RISM-KB equation. The van der Waals term V_W is the volume occupied by the van der Waals spheres representing atoms. The void volume V_V is defined as void space inside the solute molecule or at its surface that the solvent probe cannot access. In this study, the volume of voids between xenon and lysozyme is also included in the void volume. The two geometric terms V_W and V_V were calculated using the Alpha Shapes program.[24] The thermal volume V_T is defined by $\bar{V}_0 - V_{id} - (V_W + V_V)$, where $\bar{V}_0$ is the PMV of a hypothetical molecule whose atomic charges are completely removed, and thus is essentially the solvent-packing contribution of the PMV. The interaction volume V_I is defined by $\bar{V} - \bar{V}_0$ as the contribution of the electrostatic interaction between the solute and the solvent. The PMVs $\bar{V}$ and $\bar{V}_0$ are obtained from the 3D-RISM-KB theory.

2.2. PMV Calculation by the 3D-RISM-KB Theory. The PMV is calculated from the Kirkwood−Buff theory[17] extended to the 3D-RISM description[18]

$$\bar{V} = k_B T \chi_T^0 (1 - \rho \sum_\gamma \int_{V_{cell}} c_\gamma(\mathbf{r})) \quad (3)$$

where $c_\gamma(\mathbf{r})$ is the 3D direct correlation function of solvent site γ around the solute and χ_T^0 and ρ are the isothermal compressibility and the number density of pure solvent. The compressibility χ_T^0 is calculated in terms of the site−site direct correlation functions of pure solvent.[25] The first term $k_B T \chi_T^0$ in eq 3 yields the ideal volume V_{id} in eq 2.

The 3D solute−solvent correlation functions are obtained by the 3D-RISM theory.[12−15] The 3D-RISM integral equation is written as

$$h_\gamma(\mathbf{r}) = \sum_{\gamma'} c_{\gamma'}(\mathbf{r}) * (w_{\gamma'\gamma}^{vv}(r) + \rho h_{\gamma'\gamma}^{vv}(r)) \quad (4)$$

where $h_\gamma(\mathbf{r})$ is the 3D total correlation function of solvent site γ around the solute, the asterisk denotes a convolution integral in the direct space, $w_{\gamma'\gamma}^{vv}(r)$ is the intramolecular function of solvent molecules, and $h_{\gamma'\gamma}^{vv}(r)$ is the site−site total correlation function of solvent, obtained independently from a single-component RISM treatment. In this calculation, we adopt the dielectrically consistent RISM (DRISM) theory[26,27] to ensure the dielectric consistency of the solutions. The 3D-RISM equation is complemented by the 3D hypernetted-chain (HNC) closure equation, including the corrections to the 3D correlation functions for the supercell periodicity artifact[14,15]

$$h_\gamma(\mathbf{r}) = \exp(-\beta u_\gamma(\mathbf{r}) + h_\gamma(\mathbf{r}) - c_\gamma(\mathbf{r}) - \Delta Q_\gamma) + \Delta Q_\gamma - 1 \quad (5)$$

where $u_\gamma(\mathbf{r})$ is the interaction potential between solvent site γ and the whole solute, which is calculated on the supercell grid using the minimum image convention and the Ewald summation method. The correction term ΔQ_γ is given in Fourier space by

$$\Delta Q_\gamma = \frac{4\pi\beta}{V_{cell}} q \lim_{k\to 0} \sum_{\gamma'} \frac{q_{\gamma'}}{k^2} (w_{\gamma'\gamma}^{vv}(k) + \rho h_{\gamma'\gamma}^{vv}(k)) \quad (6)$$

where V_{cell} is the supercell volume, q is the net charge of the solute, and q_γ is the partial site charge of solvent site γ.

2.3. Models. Two three-dimensional structures of xenon−lysozyme complexes were constructed from the X-ray structure of the xenon−lysozyme complex[28] and the low-pressure NMR structure of lysozyme in aqueous solution.[23] The details of modeling were reported elsewhere.[22] In the model, one binding site of xenon corresponds to the binding pocket of native ligands (substrate binding site). The other site (internal site) is located in a cavity of the lysozyme. The structure of the xenon−lysozyme complex is illustrated in Figure 1.

We used the site−site pair potential consisting of the Lennard−Jones 12−6 and the Coulomb potential terms to describe the molecular interactions. The potential parameters for lysozyme atoms were taken from the AMBER (parm99) force field,[29] and for xenon from Pierotti.[30] For water, we employed the SPC/E parameters[31] with a repulsive term added to the hydrogen site[32] ($\sigma_H = 0.4$ Å and $\epsilon_H = 0.05$ kcal/mol). The parameters of the interaction between different species were obtained by the Lorentz−Berthelot mixing rules. In the Alpha Shapes calculation, Lennard−Jones potentials were replaced with hard spheres of a size chosen according to our previous study[20] to be equal to the distance at which the Lennard−Jones potential energy reaches $k_B T$. In the 3D-RISM calculation, the 3D potential $u_\gamma(\mathbf{r})$ was constructed from the site−site pair potentials. Other input data to the 3D-RISM theory

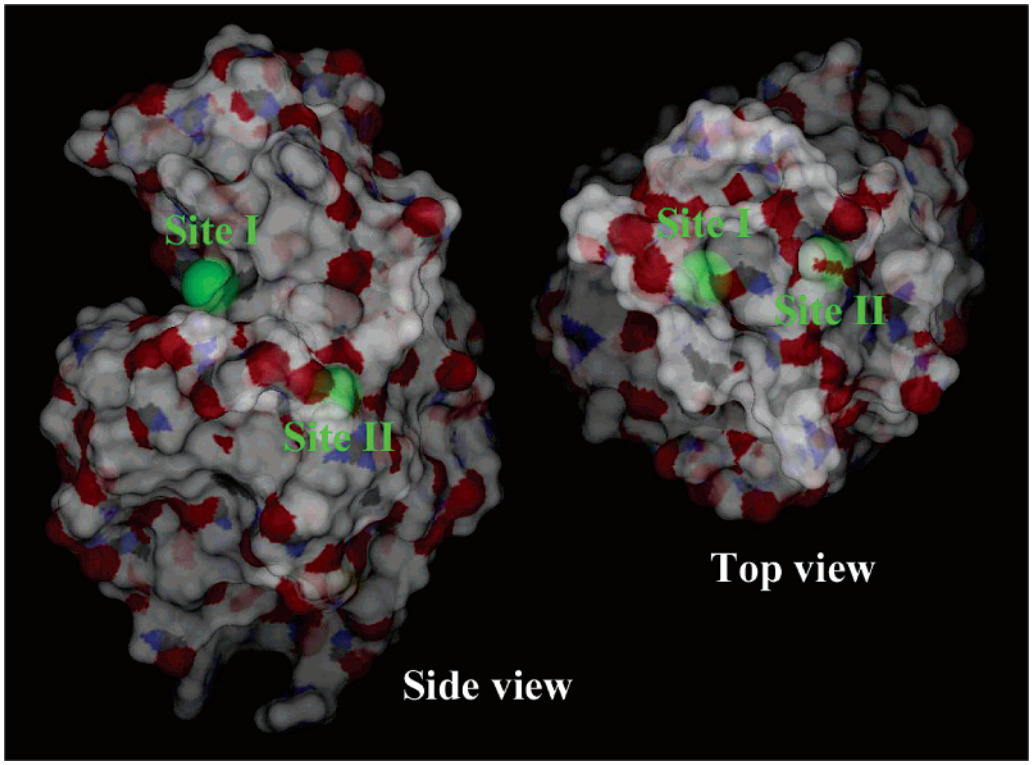

Figure 1. Structure of a xenon−lysozyme complex. Site I indicates the "substrate binding site". Site II, the "internal site", is located in a cavity of lysozyme.

TABLE 1: Partial Molar Volume $\bar{V}$ (cm³/mol) of Xenon, Lysozyme, and Two Complexes in Aqueous Solution at 298.15 K and Its Components[a]

	$\bar{V}$	V_{id}	V_W	V_V	V_T	V_I
xenon	28.6	1.3	13.7	0.0	13.6	0.0
lysozyme	9413.8	1.3	6082.4	2580.4	804.4	−54.8
xenon + lysozyme[b]	9442.4	2.7	6096.1	2580.4	818.1	−54.8
complex (substrate binding site)	9451.9	1.3	6096.1	2603.8	802.3	−51.6
$\Delta V_{binding}$[c]	9.5	−1.3	0.0	23.4	−15.7	3.2
complex (internal site)	9440.6	1.3	6096.0	2600.3	789.9	−56.0
$\Delta V_{binding}$[c]	−1.8	−1.3	0.0	19.9	−19.1	−1.2

[a] Ideal volume (V_{id}), van der Waals volume (V_W), void volume (V_V), thermal volume (V_T), and interaction volume (V_I). [b] $V_{xenon} + V_{lysozyme}$. [c] $V_{complex} - (V_{xenon} + V_{lysozyme})$.

are the number density $\rho = 0.033329$ Å^{-3}, temperature $T = 298.15$ K, and dielectric constant $\epsilon = 78.38$ of ambient water. The 3D-RISM/HNC equations were solved on a grid of 256^3 points in a cubic supercell of $(128$ Å$)^3$, using the modified direct inversion in the iterative subspace (MDIIS) method.[33]

3. Results

The first major finding of this study is that the PMV increases by 10 cm³/mol at the substrate binding site. On the basis of eq 1, this result is in concordance with the pressure reduction of the binding constant of xenon. The PMV values of xenon, lysozyme, and two complexes (in each of which one xenon atom binds to the substrate binding site or the internal site) in aqueous solution calculated using the 3D-RISM-KB theory are given in Table 1. The PMV changes accompanying the bindings, $\Delta V_{binding} = V_{complex} - (V_{xenon} + V_{lysozyme})$, are shown as well. Unlike the substrate binding site, the binding to the internal site slightly decreases or negligibly changes the PMV. It gives little pressure effect on the binding to the internal site, as follows from eq 1.

A second major finding is that the PMV increase for the substrate binding site primarily consists of a large void volume increase that is partially compensated by a decrease of the thermal volume. The volume components appearing in eq 2 are listed in Table 1. The change in the ideal volume is purely an entropic effect caused by the binding. In other words, the decrease in the ideal volume is due to the decrease of the number of molecules from 2 to 1. The latter effect is almost negligible, compared to the PMV increase. The interaction volume contributed somewhat positively. For the internal site, an increase in the void volume is almost completely compensated by a decrease in the thermal volume. The contribution of the interaction volume is negligible, too.

The PMV change associated with the binding of xenon is related to the exchange between xenon and water molecules at the site. To see the hydration change from the xenon binding to the substrate binding site, we show the radial distribution functions of water from an atomic site in the substrate binding site before and after the binding of xenon in Figure 2a. The radial distribution functions are reconstructed from the 3D distribution functions obtained by the 3D-RISM calculation. We also calculated the running coordination numbers defined by

$$N(r) = \rho \int_0^r 4\pi r'^2 g(r')\, dr' \qquad (7)$$

which are shown in Figure 2b to observe the change in the hydration number. The function represents the number of water molecules within the distance r from the origin. As seen from the figures, only within $r < 5$ Å the xenon binding has a significant effect on the hydration. The hydration number in the binding site was reduced from about 4 to 2 by the xenon binding. In other words, two water molecules were exchanged for one xenon atom. To see how the change of the hydration

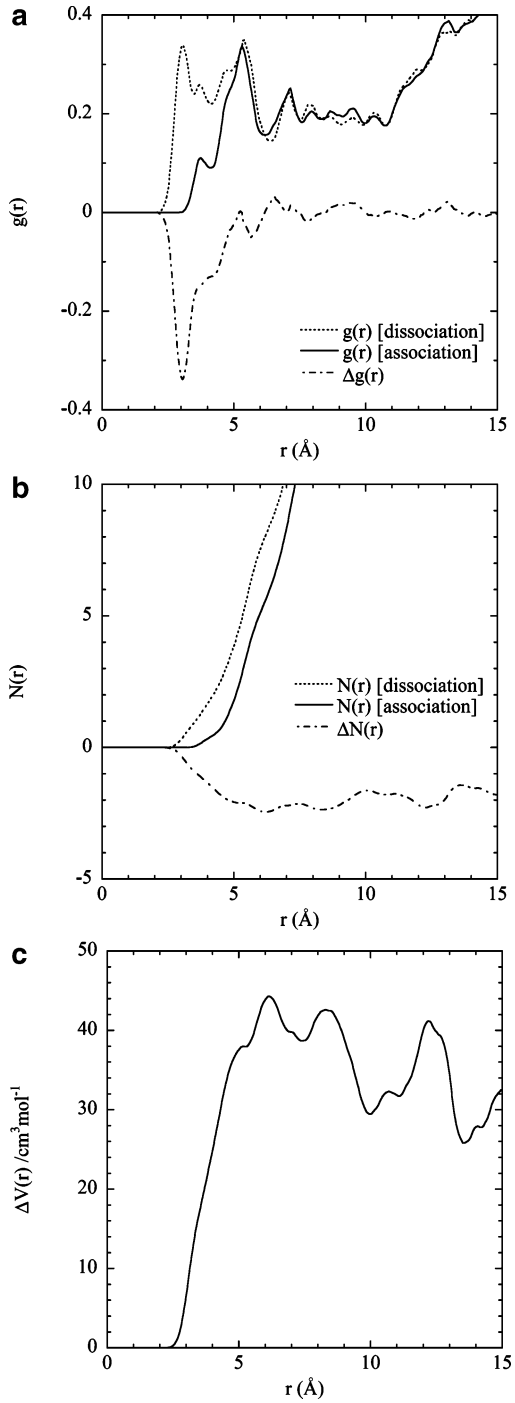

Figure 2. Radial distribution function $g(r)$, the running coordination function $N(r)$, and the local PMV function $V(r)$ viewed from the main-chain oxygen of Gln57 in the substrate binding site: (a) dotted line, $g(r)$ for lysozyme; solid line, $g(r)$ for the lysozyme−xenon complex; dot−dashed line, the difference $\Delta g(r) = g(r)$[complex] $- g(r)$-[lysozyme]; (b) dotted line, $N(r)$ for lysozyme; solid line, $N(r)$ for the lysozyme−xenon complex; dot−dashed line, the difference $\Delta N(r) = N(r)$[complex] $- N(r)$[lysozyme]; (c) the difference $\Delta V(r) = V(r)$-[complex] $- V(r)$[lysozyme].

number makes the PMV change, we use the local PMV function defined by[34,35]

$$V(r) = V_{id} - \int_0^r 4\pi r'^2 (g(r') - 1)\, dr' \qquad (8)$$

which determines the contribution of the radial distribution function $g(r)$ to the PMV within the distance r. The difference between the cases before and after the binding of xenon is shown in Figure 2c. The contribution from the binding site was about $+40$ cm^3/mol, which corresponds to the volume of two water molecules. This means the release of two water molecules makes a 40 cm^3/mol cavity that belongs to the lysozyme molecule. Thus, one xenon atom, the volume of which is 28.6 cm^3/mol (Table 1), binds to the site and expels two water molecules, $V \approx 40$ cm^3/mol, from the site. Consequently, the xenon binding increases the PMV by about 10 cm^3/mol.

The same functions for the internal site are shown in Figure 3. The xenon binding to the site affects the hydration in a somewhat more confined region, $r < 4$ Å, compared to the substrate binding site. This is simply because the internal site is separated from the outside aqueous phase. The xenon binding reduced the number of molecules within the binding site from 2 to 1. In this case, one water molecule is exchanged for one xenon atom. The volume contribution of the decrease in the hydration number is about $+20$ cm^3/mol, which is approximately the volume of one water molecule. The results exemplify that the xenon binding to the internal site only interchanges xenon and water molecules one by one, so that it does not significantly change the PMV.

4. Discussion

We have shown that the void volume change exceeds the thermal volume change for the substrate site, while they are balanced for the internal site. What is the difference between the two sites? Here, we adopt a simple molecular picture for the thermal volume: It is considered as the volume of "voids" formed between solute and solvent due to imperfect packing,[36] though it is actually a thermodynamic or hydration contribution to the PMV. When a xenon atom binds to the lysozyme site, some voids between xenon and water vanish because the xenon atom becomes partially dehydrated. Instead, some structural voids between xenon and lysozyme are created. In the same way, some voids between lysozyme and water transform to the structural voids between xenon and lysozyme. If the packing between xenon and lysozyme are similar to the packing of water, then the increase in the void volume balances the decrease in the thermal volume. The binding of xenon to the internal site expelled only one water molecule so that the voids between xenon and water and between lysozyme and water entirely transform to the structural voids between xenon and lysozyme as illustrated in Figure 4. However, at the substrate binding site two water molecules were exchanged to one xenon atom as shown above. Such an exchange makes larger voids between xenon and lysozyme as illustrated in Figure 4. Therefore, the difference of the packing between xenon and lysozyme from the packing of hydration water, or interfacial water, creates the increase in the void volume that exceeds the decrease in the thermal volume, which is the origin of the PMV increase of anesthetic binding at the molecular level.

This molecular mechanism explains why the loose binding of ligands such as anesthetics to protein sites, typically protein surfaces, expands the PMV, while the tight binding of specific ligands to their own sites does not increase the PMV or can reduce the PMV depending on the degree of packing. This is consistent with experimental results by Ueda et al.[6] that the binding of halothane (anesthetic) to luciferase increases the PMV and the binding of myristate (specific inhibitor) decreases the PMV.

The interaction volume change found in this study is directly related to the electrostriction hypothesis proposed by Eyring and Ueda.[1,4] The substrate binding site is proximate to the active site of lysozyme and has two charged residues, Glu35 and

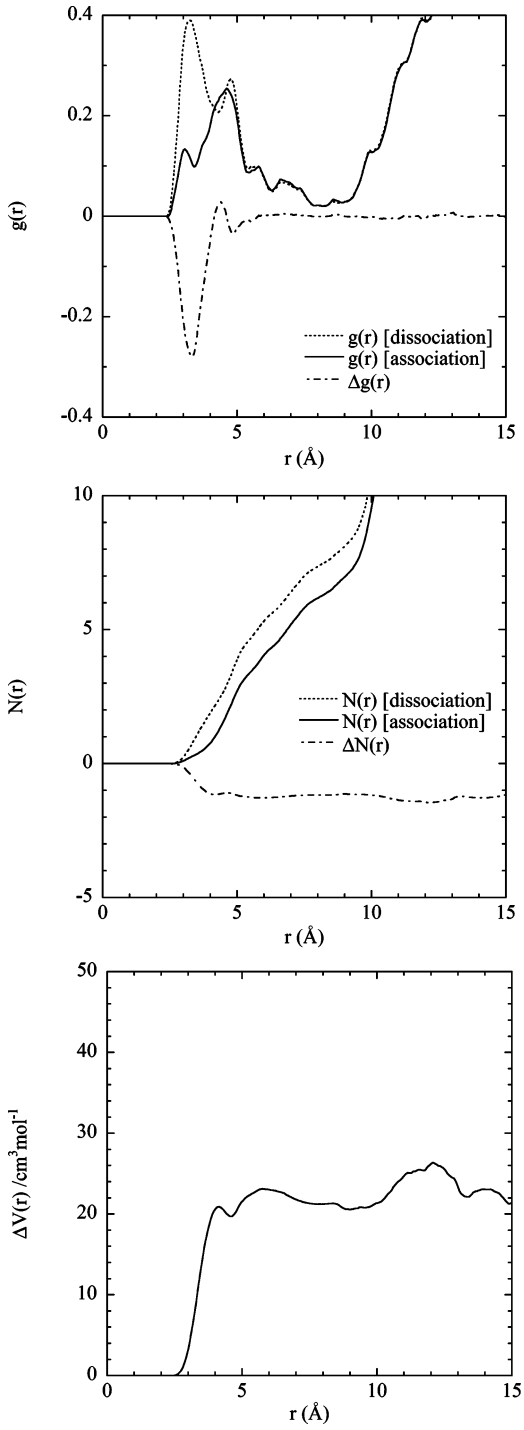

Figure 3. Radial distribution function $g(r)$, the running coordination function $N(r)$, and the local PMV function $V(r)$ viewed from the γ-carbon of Ile55 in the internal site: (a) dotted line, $g(r)$ for lysozyme; solid line, $g(r)$ for the lysozyme−xenon complex; dot−dashed line, the difference $\Delta g(r) = g(r)$[complex] − $g(r)$[lysozyme]; (b) dotted line, $N(r)$ for lysozyme; solid line, $N(r)$ for the lysozyme−xenon complex; dot−dashed line, the difference $\Delta N(r) = N(r)$[complex] − $N(r)$-[lysozyme]; (c) the difference $\Delta V(r) = V(r)$[complex] − $V(r)$-[lysozyme].

Asp52. Before a xenon atom binds to the site, the charged groups are strongly hydrated. When a xenon atom comes to the site, two water molecules are released from the site. The dehydration reduces the electrostriction. The contribution of electrostriction to the PMV is represented by the change in the interaction volume in the decomposition in eq 2, which amounts to +3.2 cm^3/mol. Our results identify and confirm the release of

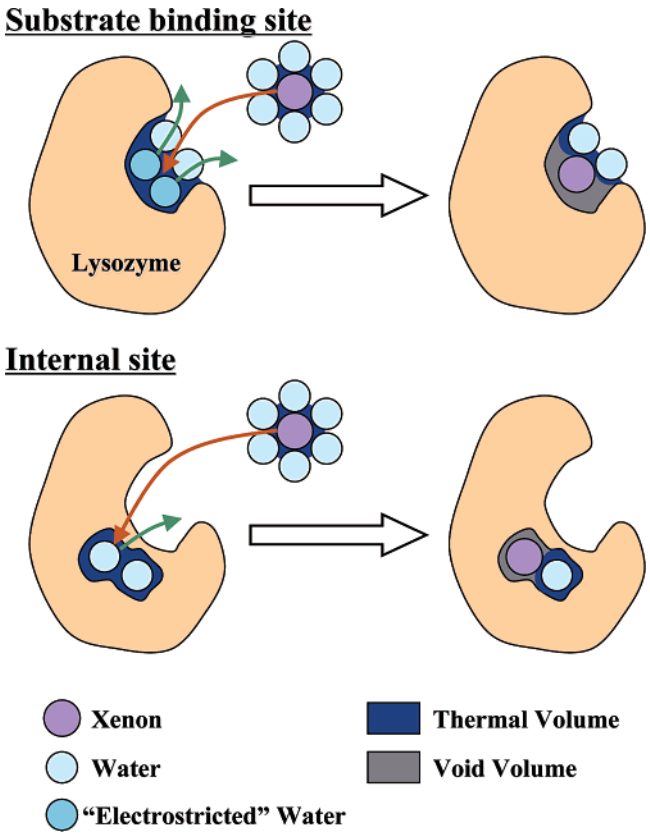

Figure 4. Illustration of the molecular mechanism of xenon−lysozyme binding and the volume change. See the text for explanation.

electrostricted water. However, the electrostricted water release is found to be a secondary contribution to the PMV increase, which will cause pressure reversal of anesthesia.

For the internal site, the interaction volume change is almost negligible. This is reasonable from the following viewpoint. The water molecules confined in the cavity are isolated from bulk water. In such cases, the detailed hydration structure does not affect the interaction volume and the PMV, because it is determined by the volume of the cavity when the number of water molecules is unchanged regardless whether the cavity is hydrophilic or hydrophobic (it is actually hydrophobic). If the number of water molecules were increased by strong interactions between the cavity sites and water molecules, then the contribution of the interaction volume would be reduced in a similar way to the electrostriction.

Finally, we should refer to the quantitative aspects of the PMV change. The PMV increase by 10 cm^3/mol accompanying the xenon−lysozyme binding in this study is far different from an experimental result for the diethyl ether−albumin binding, which shows 295 cm^3/mol expansion of the PMV.[4] There are two possible explanations for the discrepancy. First, the binding of anesthetics could change the PMV of the protein by modifying the protein structure, though the xenon−lysozyme binding does not substantially change the protein structure.[28] Considering such structural changes is the next step to complete elucidation of the molecular mechanism of the pressure effect on anesthetic−protein binding. Second, the discrepancy can come from the difference of the number of anesthetic molecules interacting with protein. In our model, we assumed that only a few xenon atoms bind to lysozyme because docking simulations as well as X-ray analysis could detect only a few binding sites that are energetically distinguished from others. However, a large number of anesthetic molecules, including ones quite weakly or occasion-

ally binding to protein, may interact with the protein surface and perturb the PMV at real surgical concentrations. Therefore, it is necessary to take such molecules into account to more precisely estimate the value of the PMV change. The 3D-RISM theory can be also applied to the detection of such molecules in terms of the distribution functions of cosolvent as well as solvent.[37] Such studies are now in progress in our group.

5. Conclusion

We found that the binding of xenon to the substrate binding site of lysozyme increased the PMV by 10 cm^3/mol. The xenon binding released two water molecules from the site. The consequent PMV increase was mainly due to the creation of additional voids resulting from the loose binding of xenon to the site. The inhibition of electrostriction was a minor contribution to the PMV increase. The results imply that the pressure reversal of general anesthesia can be caused by loose packing between the anesthetics and the action site.

Acknowledgment. This work was supported in part by Grant-in-Aids for Scientific Research on the Priority Area of "Water and Biomolecules" and for the NAREGI Nanoscience Project from the Japanese Ministry of Education, Culture, Sports, Science and Technology (MONBUKAGAKUSHO). T.I. is also grateful for the support by a Grant-in-Aid for Young Scientists from the Ministry. T.S. is thankful for the support of a Fundamental Research (C) Grant-in-Aid for Scientific Research from the Ministry.

References and Notes

(1) Eyring, H.; Woodbury, J. W.; D'Arrigo, J. S. *Anesthesiology* **1973**, *38*, 415.
(2) Miller, K. W.; Paton, W. D. M.; Smith, R. A.; Smith, E. B. *Mol. Pharmacol.* **1973**, *9*, 131.
(3) Franks, N. P.; Lieb, W. R. *Nature* **1982**, *300*, 487.
(4) Ueda, I.; Mashimo, T. *Physiol. Chem. Phys.* **1982**, *14*, 157.
(5) Moss, G. W. J.; Lieb, W. R.; Franks, N. P. *Biophys. J.* **1991**, *60*, 1309.
(6) Ueda, I.; Matsuki, H.; Kamaya, H.; Krishna, P. R. *Biophys. J.* **1999**, *76*, 483.
(7) Franks, N. P.; Lieb, W. R. *Nature* **1994**, *367*, 607.
(8) Miller, K. W. *Br. J. Anaesth.* **2002**, *89*, 17.
(9) Campagna, J. A.; Miller, K. W.; Forman, S. A. *N. Engl. J. Med.* **2003**, *348*, 2110.
(10) Millero, F. J. *Chem. Rev.* **1971**, *71*, 147.
(11) Chalikian, T. V.; Breslauer, K. J. *Biopolymers* **1996**, *39*, 619.
(12) Beglov, D.; Roux, B. *J. Phys. Chem.* **1997**, *101*, 7821.
(13) Kovalenko, A.; Hirata, F. *Chem. Phys. Lett.* **1998**, *290*, 237.
(14) Kovalenko, A.; Hirata, F. *J. Chem. Phys.* **2000**, *112*, 10391.
(15) Kovalenko, A. In *Molecular Theory of Solvation*; Hirata, F., Ed.; Kluwer: Dordrecht, The Netherlands, 2003; p 169.
(16) Imai, T.; Kovalenko, A.; Hirata, F. *Chem. Phys. Lett.* **2004**, *395*, 1.
(17) Kirkwood, J. G.; Buff, F. P. *J. Chem. Phys.* **1951**, *19*, 774.
(18) Harano, Y.; Imai, T.; Kovalenko, A.; Kinoshita, M.; Hirata, *J. Chem. Phys.* **2001**, *114*, 9506.
(19) Imai, T.; Harano, Y.; Kovalenko, A.; Hirata, F. *Biopolymers* **2001**, *59*, 512.
(20) Imai, T.; Kovalenko, A.; Hirata, F. *J. Phys. Chem. B* **2005**, *109*, 6658.
(21) Imai, T.; Takekiyo, T.; Kovalenko, A.; Hirata, F.; Kato, M.; Taniguchi, Y. *Biopolymers* **2005**, *79*, 97.
(22) Isogai, H.; Seto, T.; Nosaka, S. *Int. Congr. Ser.* **2005**, *1283*, 318.
(23) Refaee, M.; Tezuka, T.; Akasaka, K.; Williamson, M. P. *J. Mol. Biol.* **2003**, *327*, 857.
(24) Edelsbrunner, H.; Facello, M.; Fu, P.; Liang, J. In *Proceedings of the 28th Annual Hawaii International Conference on System Science*; IEEE Computer Society Press: Los Alamitos, CA, 1995; Vol. 5, p 256.
(25) Imai, T.; Kinoshita, M.; Hirata, F. *J. Chem. Phys.* **2000**, *112*, 9469.
(26) Perkyns, J. S.; Pettitt, B. M. *Chem. Phys. Lett.* **1992**, *190*, 626.
(27) Perkyns, J.; Pettitt, B. M. *J. Chem. Phys.* **1992**, *97*, 7656.
(28) Prangé, T.; Schiltz, M.; Pernot, L.; Colloc'h, N.; Longhi, S.; Bourguet, W.; Fourme, R. *Proteins* **1998**, *30*, 61.
(29) Wang, J. M.; Cieplak, P.; Kollman, P. A. *J. Comput. Chem.* **2000**, *21*, 1049.
(30) Pierotti, R. A. *J. Phys. Chem.* **1965**, *69*, 281.
(31) Berendsen, H. J. C.; Grigera, J. R.; Straatsma, T. P. *J. Phys. Chem.* **1987**, *91*, 6269.
(32) Pettitt, B. M.; Rossky, P. J. *J. Chem. Phys.* **1982**, *77*, 1451.
(33) Kovalenko, A.; Ten-no, S.; Hirata, F. *J. Comput. Chem.* **1999**, *20*, 928.
(34) Matubayasi, N.; Levy R. M. *J. Phys. Chem.* **1996**, *100*, 2681.
(35) Imai, T.; Nomura, H.; Kinoshita, M.; Hirata, F. *J. Phys. Chem. B* **2002**, *106*, 7308.
(36) Terasawa, S.; Itsuki, H.; Arakawa, S. *J. Phys. Chem.* **1975**, *79*, 2345.
(37) Imai, T.; Hiraoka, R.; Kovalenko, A.; Hirata, F. *J. Am. Chem. Soc.* **2005**, *127*, 15334.